Nanostructure Transformation

DOI: 10.1002/anie.200701553

# Disassembly and Self-Reassembly in Periodic Nanostructures: A Face-Centered-to-Simple-Cubic Transformation**

*Fan Li, Sarah A. Delo, and Andreas Stein**

Crystallization of uniform colloids into extended three-dimensional structures other than the trivial face-centered-cubic (*fcc*) lattice that resembles natural opals remains a challenge of nanomaterials synthesis.[1] The few successful approaches have required careful balance of electrostatic interactions between nanoparticles. Herein, we describe a different approach to a relatively rare colloidal crystal structure, a three-dimensional simple-cubic nanoparticle array. The method relies on structural memory effects related to a *fcc* colloidal crystal template. A $TiO_2$–$P_2O_5$ binary structure was prepared by combined surfactant templating and colloidal crystal templating with a polymer opal. During calcination, the initially formed inverted opal structure disassembled into nanocubes and smaller spheroids. After assimilation of the spheroids by the cubes, the latter self-reassembled into simple-cubic arrays (Scheme 1). This template-directed approach may become a general way for creating periodic nanostructures with simple cubic symmetries and perhaps other symmetries as well. It provides a new avenue for designing nanostructures relevant to photonic, optoelectronic, and other applications.

Unique materials properties can be achieved by scaling down particle dimensions to the nanometer regime. In many advanced applications involving nanoparticles, it is necessary to assemble them into arrays with a specific architecture. For such arrays, interesting optical, magnetic, or catalytic properties may arise from interactions between nanoparticles or from other effects of the larger, collective structure.[2,3] Colloidal crystals are examples of periodic nanoparticle arrays. These have been employed as photonic crystal structures and as templates to produce negative replica structures of the colloidal crystals (e.g., inverted opals).[4–6] Materials properties, including photonic band structures, depend on the specific geometry of the colloidal crystal. Colloidal crystals prepared by natural assembly of uniform spherical particles form close-packed arrays, typically with *fcc* packing.[7] Other three-dimensional packing motifs are more difficult to obtain.[8] Small colloidal clusters of unusual symmetric patterns can be achieved within two- or three-dimensional confinement.[9,10] A limited number of layers of non-close-packed colloidal crystals have been formed by convective assembly on a patterned substrate that directs the crystal geometry at the interface.[11] Recent successes in achieving non-close packed colloidal crystals have relied on a delicate balance of electrostatic interactions in binary particle systems.[1,12] However, less intricate, perhaps more-general assembly strategies are desirable and would introduce materials design tools for an even wider range of applications. In the past few years, various inorganic superstructures composed of nanoparticles with orientational order (mesocrystals) have been prepared by self-assembly of faceted nanoparticles.[13] Our approach of preparing periodic arrays of uniform nanoparticles is based on a new concept of combining disassembly (top down) and self-reassembly (bottom up) syntheses. In the reassembled colloidal crystals, simple-cubic packing, which is relatively rare even among atomic crystals, extends in three-dimensions over a large number of unit cells.

The unusual colloidal crystal growth process builds on a method that was recently introduced by our group to synthesize uniform, shaped silica nanoparticles through combined templating and disassembly processes.[14] By replicating the void structure in a predominantly *fcc* colloidal crystal of poly(methylmethacrylate) (PMMA) spheres, a

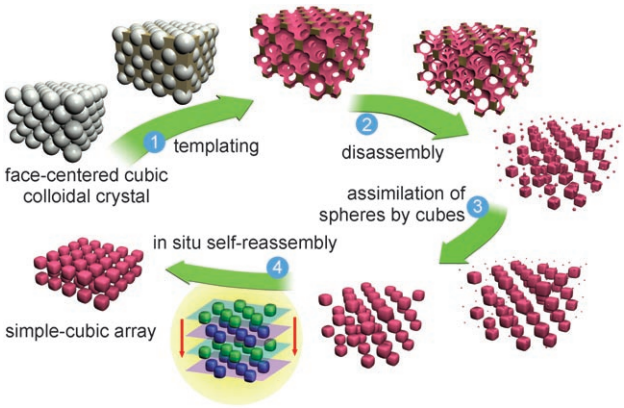


***Scheme 1.*** Schematic of the proposed disassembly and self-reassembly mechanism in situ. A porous skeleton is templated by a face-centered-cubic colloidal crystal and disassembles into its building blocks during calcination. Smaller particles are assimilated by the larger cubes. Alternating layers of cubes merge, driven by capillary forces from a melted phase, producing the observed simple-cubic-packed arrays of nanocubes. For clarity, the interparticle space is exaggerated and any irregular aggregates are ignored.

[*] F. Li, S. A. Delo, Prof. A. Stein
Department of Chemistry
University of Minnesota
Minneapolis, MN 55455 (USA)
Fax: (+1) 612-626-7541
E-mail: stein@chem.umn.edu

[**] This work was financially supported by the Petroleum Research Foundation, administered by the American Chemical Society (ACS-PRF grant number 42751-AC10), and in part by the MRSEC program of the NSF (DMR-0212302), which supports the University of Minnesota Characterization Facility. The authors thank Rick A. Knurr for elemental analysis and Dr. Joysurya Basu for assistance with Z-contrast imaging and elemental mapping.

Supporting information for this article is available on the WWW under http://www.angewandte.org or from the author.

three-dimensionally ordered macroporous (3DOM) structure with the same symmetry was initially obtained, which under controlled conditions spontaneously disassembled into individual particles by fracturing at interconnecting necks (see the Supporting Information). As the *fcc* colloidal crystal molded the characteristic 3DOM or inverse opal structure, it also dictated the shape and size of the nanoparticles obtained after disassembly. We have now successfully applied this strategy to the syntheses of various metal oxide particles. Strikingly, we discovered that in certain systems, templated nanoparticles reassembled into colloidal crystals with new symmetries. A particularly interesting composition consists of the semiconductor titania precipitated within a $P_2O_5$ glass phase.[15–18] Starting from titanium isopropoxide and triethylphosphate precursors with Brij 56 as an additive intended to induce mesoporosity and acetylacetone (*acac*) as a complexing agent for titanium ions, bimodally dispersed $TiO_2$–$P_2O_5$ nanocubes and spheres were obtained after calcination of the PMMA–template/precursor composite. Figure 1a shows a scanning electron microscopy (SEM) image of a typical product obtained in the dual-templated $TiO_2$–$P_2O_5$ system. Three distinct regions with different morphologies can be observed. In region A, nanoparticles are connected at corners to form a macroporous skeleton whose symmetry resembles that of the original template, an *fcc* colloidal crystal formed from monodisperse PMMA spheres. This area corresponds to a synthesis stage in which the solid occupying the interstitial regions of the original template remains continuous, that is, the stage typically targeted for the design of 3DOM structures or inverse opals. In region B, the replica structures of the octahedral and tetrahedral holes in the *fcc* template became disconnected and the resulting nanocubes and smaller nanospheres occupy random positions with random orientations. This situation corresponds with our observations in the previously studied silica system.[14] Most of the sample (approximately 60–80%, depending on the specimen), however, resembles the structure in region C. Here, nanocubes are arranged periodically, forming layers with square packing. A closer analysis of an ordered region reveals a structure with a largely simple-cubic packing symmetry (Figure 1b–d). In the five adjacent layers shown in Figure 1b, rows of partially rounded cubes lie on top of each other and are oriented nearly parallel to each other. The degree of alignment perpendicular to the layer direction is also high, as is apparent from the good match with a 3D model of a simple-cubic lattice (Figure 1c, d). A few point or line defects are observed within layers, but misorientation between layers is relatively small. None of the smaller nanoparticles are observed in this region. Such structural order extends over a much larger range (see the Supporting Information).

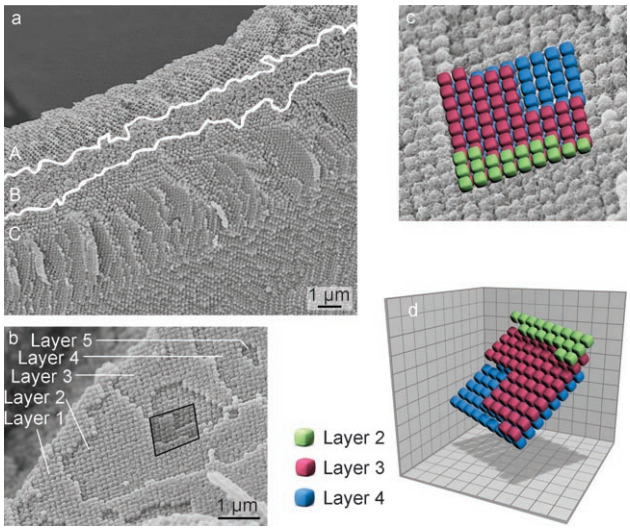


***Figure 1.*** a) SEM image of a $TiO_2$–$P_2O_5$ sample ($Ti/H_2O$ molar ratio = 1:1.8) prepared by disassembly–reassembly reactions in situ. The image shows a region in which connected nanocubes surround void spaces originating from the original *fcc* colloidal crystal template (A), a region in which disconnected nanocubes and nanospheres occupy random positions with random orientations (B), and the largest region with simple-cubic packing of nanocubes (C), which is representative of approximately 70–80% of this sample. b) SEM image of an ordered area of nanocubes from region C. Five discrete layers can be seen with square packing of cubes within each layer. c) An expanded view of the outlined region from (b) with an overlay of cubes to illustrate the simple-cubic packing in this region. d) A three-dimensional plot of the three layers from (c) to illustrate the stacking of layers in a simple-cubic geometry.

To understand the mechanism for formation of the simple-cubic array structure, it is necessary to analyze the building blocks at various stages of reassembly. Figure 2a is an SEM image of a region similar to region B. Cubes with edge lengths of approximately $115 \pm 4$ nm and spheroids with diameters of approximately $62 \pm 4$ nm were produced by using a template of $(378 \pm 7)$-nm diameter, closest-packed PMMA spheres. These particles have well-defined morphologies and remain unagglomerated. The geometrical relationship between the initial 3DOM structure and the isolated cubes and spheres has been explained previously.[14] In short, the cubes originate from octahedral voids surrounded by six templating PMMA spheres, and the spheroids arise from the tetrahedral interstices formed among four spheres. Therefore, their shapes and sizes are determined by the PMMA template, which provides facile control over the morphology and reproducibility. In addition to cubes and spheroids, some minute irregular particles (approximately 10 nm) are observed. These are believed to originate from ion diffusion processes that occur during calcinations, but after removal of the PMMA template, because longer calcination times produced more of these irregular particles. Some necks were retained in the disassembly, producing chains and larger arrays of connected cubes and spheroids (Figure 2b, c) and providing evidence that the particles evolved from the 3DOM structure. The nanocubes and spheroids possess a vermicular mesostructure templated from the Brij 56 nonionic surfactant, as visualized in the transmission electron microscopy (TEM) image (Figure 2d). For a sample prepared with a low water content ($H_2O/Ti$ mole ratio = 1.8), only faint diffraction rings can be seen in the selective area electron diffraction (SAED) image, indicating that an amorphous phase dominated the structure. In the small-angle X-ray scattering (SAXS) pattern of this sample, only a weak, broad reflection centered around 6.0 nm was observed, which is consistent with a wormlike mesostructure. Even though a nonionic surfactant was employed in

  

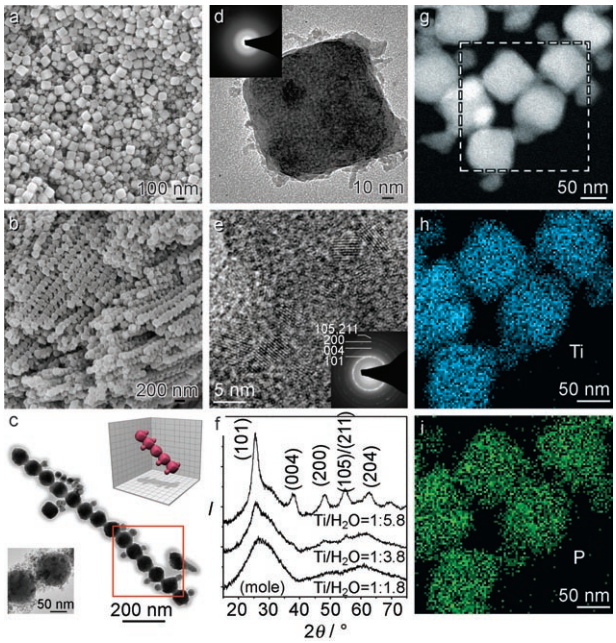


***Figure 2.*** a) SEM image of cubic and spheroidal nanoparticles obtained by disassembly of 3DOM $TiO_2$–$P_2O_5$ (region B in Figure 1 a). b) SEM image of arrays of $TiO_2$–$P_2O_5$ nanoparticles in which the smaller spheroids originating from tetrahedral holes are still visible. c) TEM image of a one-dimensional chain of rounded cubes together with smaller nanoparticles. The expanded region shows a halo of minute particles around the larger nanoparticles. The schematic diagram provides a three-dimensional interpretation of this structure. d) TEM image of a cubic nanoparticle prepared with a $Ti/H_2O$ molar ratio of 1:1.8 (inset: SAED pattern). e) HRTEM image of a $TiO_2$–$P_2O_5$ nanoparticle prepared with a $Ti/H_2O$ molar ratio of 1:5.8, which produced crystalline anatase nanoparticles within a glassy $P_2O_5$ matrix (inset: SAED pattern). f) A comparison of X-ray powder diffraction patterns for two samples prepared with $Ti/H_2O$ molar ratios of 1:1.8 (bottom), 1:3.8 (middle), and 1:5.8 (top). The degree of titania crystallization increased with higher water content. g) High-angle angular dark field scanning transmission electron microscopy (HAADF-STEM) image of particles in a sample prepared with a $Ti/H_2O$ molar ratio of 1:5.8. h) Ti mapping of the outlined region in (g). i) P mapping of the outlined region in (g). Note that samples in (c), (g), (h), and (i) were prepared with a template composed of smaller PMMA spheres than in the other samples shown.

this synthesis, a relatively low BET (Brunauer–Emmett–Teller) surface area of 83.0 $m2\,g^{-1}$ and a mesopore volume of 0.085 $cm3\,g^{-1}$ were measured by nitrogen adsorption. These low values are attributed to a combination of three factors: partial collapse of mesopores during calcination, incomplete removal of the surfactant template (samples prepared at 400 °C were not completely white),[19] and blocking of mesopore openings as smaller spheroids were assimilated by the cubes (see discussion below). Elemental analysis revealed that the P content in the product (44.6 wt % Ti, 10.7 wt % P, corresponding to a molar ratio of 2.68:1) was lower than in the precursor mixture (Ti/P molar ratio of 2:1). This reduction indicates that some phosphate was not retained in the matrix, possibly owing to its lower hydrolytic reactivity[20] or to partial sublimation of the $P_2O_5$ glass phase during calcination. With a higher water content ($H_2O$/Ti molar ratios up to 5.8:1), the fraction of crystalline $TiO_2$ (anatase) grew, but the particle shape was still well preserved (see TEM image and SAED pattern in Figure 2 e and powder X-ray diffraction (XRD) patterns in Figure 2 f). These anatase domains were embedded in an amorphous $P_2O_5$ phase to form the larger cubes containing Ti and P atoms throughout (determined by elemental mapping; Figure 2 g–i).

Formation in situ of the ordered simple-cubic structure can now be explained as follows (see Scheme 1). The initial steps are analogous to processes observed in the disassembly of 3DOM silica with mesoporous walls.[14] During calcinations, the walls of the 3DOM structure become thinner and the connected skeleton transforms to discrete particles of two different sizes (Figure 2 a). With prolonged calcination, the edges and corners of the kinetically stabilized nanoparticles become more rounded to minimize surface energies. At the calcination temperature, further structural transformation may occur through sintering and Ostwald ripening processes in the phosphate-containing medium.[21,22] The smaller particles arising from tetrahedral interstices are more susceptible to shrinkage because of their (originally) more extended shapes and smaller volumes.[14] As the spheres are assimilated by the larger cubes, only cubes are left as recognizable shapes. As expected from such a process, the final cubes are larger than their original cubic precursors ($(134 \pm 7)$ nm in region C (Figure 1 b) compared with $(115 \pm 4)$ nm in region B (Figure 2 a)). Figure 2 b shows a region in the sample where smaller spheres are still present, but some of these appear to combine with the cubes. When the smaller spheres are largely eliminated, a structural reorganization of the discrete nanocubes can occur. In the 3DOM structure, the octahedral units considered by themselves are in an *fcc* arrangement. Along the [001] direction, uniformly oriented cubes on every two adjacent *fcc* layers occupy complementary positions. Therefore, adjacent layers of the originally *fcc* structured nanocubes may interpenetrate and collapse to restack in a regular fashion, forming the simple-cubic lattice. An animated cartoon of the reassembly in situ is provided in the Supporting Information. This reassembly process may be concurrent with the disassembly, leading to the three different packing regions (Figure 1 a) and the occurrence of some cubic arrays in which smaller spheroidal particles are still present (Figure 2 b).

Such ordered simple-cubic arrays with low packing densities and sixfold coordination have not been achieved through natural self-assembly except when a patterned substrate was used.[11] Indeed, although cubic nanoparticles prefer a square pattern in 2D,[23] periodic assembly in 3D is not normally favored owing to the energy barrier for cube reorientation. In our case, the simple-cubic packing is dictated by the placement of nanocubes as a result of using an *fcc* template and facilitated by larger contact areas in rounded cubes compared with hard spheres. The driving force for self-reassembly is likely to involve capillary forces, facilitated by a low melting, relatively mobile phase; in this case, the phosphate-rich phase. To date, we have not observed reformed colloidal crystals in a phosphate-free titania system or in a pure-silica system, but we have found regions of simple-cubic assemblies in a related $ZrO_2$–$P_2O_5$ system. The need for a liquid-forming phase to facilitate reassembly may also explain the observation of the disordered region

  

(region B in Figure 1a) near the external surface of the aggregate, where phosphate is more-easily lost through sublimation. With insufficient phosphate, capillary forces may have been too weak to cause self-reassembly. It is notable that after redispersion of the assembled cube arrays through sonication and subsequent resedimentation, no structural ordering could be observed, indicating that the predefined position and orientation are indispendible in the process in situ.

In summary, we report herein a template-directed synthesis of bimodally dispersed $TiO_2$–$P_2O_5$ nanocubes and spheroids, which are transformed into extended 3D simple-cubic arrays of a single type of nanoparticle through a nonelectrostatic, self-reassembly process in situ. The mechanism in this unusual transformation from *fcc* to simple-cubic arrays relies on the special positioning and orientation of template-confined nanoparticles and may occur in parallel with the disassembly process. Many applications involving colloidal crystals (photonics,[9] optoelectronics,[24] combinatorial screening,[25] etc.) depend on the specific geometry of the colloidal crystal and/or on interactions between colloidal particles. This unique approach to simple-cubic arrays of nanoparticles adds to the choices of available geometries, coordination numbers, and packing densities in nanoparticle arrays. Even though the structures created in the present work are far away from the perfection necessary for photonic crystals, an adaptation of the self-reassembly method may provide a faster, low-cost alternative to produce simple-cubic photonic crystals that are normally prepared by elaborate micromachining, layer-by-layer lithography, holography, and macroporous silicon etching, all of which are expensive and time-consuming methods.[26–29] The simple-cubic colloidal crystals may also serve as templates to produce inverted photonic crystal structures with this geometry. Following the strategy presented herein, it may be possible to alter nanoparticle shapes and achieve more-complex geometries in colloidal crystal systems through combined disassembly and self-reassembly processes.

Received: April 9, 2007
Revised: June 8, 2007
Published online: July 30, 2007

**Keywords:** colloidal crystals · nanomaterials · self-assembly · sol–gel process · template synthesis

[1] A. M. Kalsin, M. Fialkowski, M. Paszewski, S. K. Smoukov, K. J. M. Bishop, B. A. Grzybowski, *Science* **2006**, *312*, 420.
[2] S. A. Maier, P. G. Kik, H. A. Atwater, S. Meltzer, E. Harel, B. E. Koel, A. A. G. Requicha, *Nat. Mater.* **2003**, *2*, 229.
[3] J. Hoinville, A. Bewick, D. Gleeson, R. Jones, O. Kasyutich, E. Mayes, A. Nartowski, B. Warne, J. Wiggins, K. Wong, *J. Appl. Phys.* **2003**, *93*, 7187.
[4] A. Blanco, E. Chomski, S. Grabtchak, M. Ibisate, S. John, S. W. Leonard, C. Lopez, F. Meseguer, H. Miguez, J. P. Mondia, G. A. Ozin, O. Toader, H. M. van Driel, *Nature* **2000**, *405*, 437.
[5] Y. A. Vlasov, X. Z. Bo, J. C. Sturm, D. J. Norris, *Nature* **2001**, *414*, 289.
[6] P. Lodahl, A. F. van Driel, I. S. Nikolaev, A. Irman, K. Overgaag, D. Vanmaekelbergh, W. L. Vos, *Nature* **2004**, *430*, 654.
[7] H. Míguez, F. Meseguer, C. López, A. Mifsud, J. S. Moya, L. Vázquez, *Langmuir* **1997**, *13*, 6009.
[8] O. D. Velev, *Science* **2006**, *312*, 376.
[9] Y. Yin, Y. Xia, *Adv. Mater.* **2001**, *13*, 267.
[10] V. N. Manoharan, M. T. Elsesser, D. J. Pine, *Science* **2003**, *301*, 483.
[11] J. P. Hoogenboom, C. Retif, E. de Bres, M. van de Boer, A. K. Van Langen-Suurling, J. Romijn, A. van Blaaderen, *Nano Lett.* **2004**, *4*, 205.
[12] M. E. Leunissen, C. G. Christova, A. P. Hynninen, C. P. Royall, A. I. Campbell, A. Imhof, M. Dijkstra, R. van Roij, A. van Blaaderen, *Nature* **2005**, *437*.
[13] H. Cölfen, M. Antonietti, *Angew. Chem.* **2005**, *117*, 5714; *Angew. Chem. Int. Ed.* **2005**, *44*, 5576, and references therein.
[14] F. Li, Z. Wang, A. Stein, *Angew. Chem.* **2007**, *119*, 1917; *Angew. Chem. Int. Ed.* **2007**, *46*, 1885.
[15] D. Li, H. Zhou, I. Honma, *Nat. Mater.* **2004**, *3*, 65.
[16] M. Thieme, F. Schüth, *Microporous Mesoporous Mater.* **1999**, *27*, 193.
[17] A. Bhaumik, S. Inagaki, *J. Am. Chem. Soc.* **2001**, *123*, 691.
[18] J. Zhao, B. Tian, Y. Yue, W. Hua, D. Zhao, Z. Gao, *J. Mol. Catal. A* **2005**, *242*, 218.
[19] F. Kleitz, W. Schmidt, F. Schüth, *Microporous Mesoporous Mater.* **2001**, *44–45*, 95.
[20] M. Zaharescu, A. Vasilescu, V. Badescu, M. Radu, *J. Sol-Gel Sci. Technol.* **1997**, *8*, 59.
[21] H. G. Yang, H. C. Zeng, *J. Phys. Chem. B* **2004**, *108*, 3492.
[22] J. Schmidt, W. Vogelsberger, *J. Phys. Chem B* **2006**, *110*, 3955.
[23] S. Yamamuro, K. Sumiyama, *Chem. Phys. Lett.* **2006**, *418*, 166.
[24] F. Fleischhaker, R. Zentel, *Chem. Mater.* **2005**, *17*, 1346.
[25] M. Trau, B. J. Battersby, *Adv. Mater.* **2001**, *13*, 975.
[26] S.-Y. Lin, J. G. Fleming, R. Lin, M. M. Sigalas, R. Biswas, K. M. Ho, *J. Opt. Soc. Am. B* **2001**, *18*, 32.
[27] S. Venkataraman, G. J. Schneider, J. Murakowski, S. Shi, D. W. Prather, *Appl. Phys. Lett.* **2004**, *85*, 2125.
[28] J. H. Moon, S. Yang, S.-M. Yang, *Appl. Phys. Lett.* **2006**, *88*, 121101/1.
[29] S. Matthias, R. Hillebrand, F. Muller, U. Gosele, *J. Appl. Phys.* **2006**, *99*, 113102/1.

  